Reports of Biochemistry & Molecular Biology
Vol.12, No.3, Oct 2023

Original article

www.RBMB.net

Impact of Cerium Oxide Nanoparticles on Metabolic, Apoptotic, Autophagic and Antioxidant Changes in Doxorubicin-Induced Cardiomyopathy: Possible Underlying Mechanisms

Shorouk Elsaeed Mohammed Elmorshdy[1], Gehan Ahmed Shaker[1], Zienab Helmy Eldken[1,2], Mahmoud Abdelbadie Salem[3], Amira Awadalla[4], Hany Mahmoud Abdel Shakour[3], Mohammed Elmahdy El Hosiny Sarhan[1], Abdelaziz Mohamed Hussein*[1]

Abstract

Background: In the current study, the effects of cerium oxide nanoparticles (nanocerium; NC) on doxorubicin (DOX)-induced cardiomyopathy and its possible underlying mechanisms were addressed.
Methods: 32 adult male rats were allocated into 4 groups; i) control group, ii) NC group; rats received NC (0.2 mg/kg, i.p., daily), iii) DOX group; rats received DOX 4 mg/kg (2 injections with a 14-day interval), and iv) DOX+NC group as DOX but rats received NC. At the end of the experiment, ECG and ECHO recordings and assessments of the levels of cardiac enzymes (CK-MB, LDH), and myocardial oxidative stress (MDA, catalase, and GSH), the expression of LC3 and beclin1 (markers of autophagy), caspase3 (marker of apoptosis) by immunohistochemistry, the expression of acetyl-CoA carboxylase alpha (ACCA) by PCR, and 5'adenosine monophosphate-activated protein kinase (AMPK) levels in the heart tissues were performed.
Results: The DOX group displayed a prolonged corrected QT interval, an increase in cardiac enzymes (CK-MB and LDH), myocardial oxidative stress (high MDA with low catalase and GSH), expression of ACCA, caspase-3, beclin1, and LC3 in myocardial tissues, with reduction in myocardial AMPK levels, and myocardial contractility (low ejection fraction, and fractional shortening). On the other hand, administration of NC with DOX resulted in significant improvement of all studied parameters.
Conclusions: NC offers a cardioprotective effect against DOX-induced cardiomyopathy. This effect might be due to its antioxidant and antiapoptotic effects as well as to the modulation of autophagy and metabolic dysfunctions induced by DOX in the heart tissues.

Keywords: Autophagy, Cardiomyopathy, Cerium oxide nanoparticles, Doxorubicin, Echocardiography, Oxidative stress.

Introduction

A variety of heart diseases known as cardiomyopathies usually cause progressive heart failure and high rates of morbidity and mortality due to anatomical, pathological, or

1: Medical physiology department, Faculty of Medicine, Mansoura University, Egypt.
2: Department of Basic Medical Sciences, Ibn Sina University for Medical Sciences, Amman11104, Jordan.
3: Department of cardiology, Mansoura Faculty of Medicine, Mansoura university, Egypt.
4: Center of Excellence for Genome and Cancer Research, Urology and Nephrology Center, Mansoura University, Mansoura, 35516, Egypt.
***Corresponding author: Abdelaziz Mohamed Hussein; Tel: +20 1002421140; E-mail: menhag@mans.edu.eg.**
Received: 27 Jun, 2023; Accepted: 7 Aug, 2023

[DOI: 10.61186/rbmb.12.3.495]

electrical dysfunctions of cardiac muscle (1). These cardiomyopathies may be caused by a primary myocardial illness or occur as subsequent to a number of circumstances, such as myocardial ischemia, inflammation, infection or exposure to toxic substances (2). Doxorubicin (DOX), a common chemotherapeutic agent for cancers in adults and children, results in cardiotoxicity which limits its use in cancer patients (3). DOX-induced cardiotoxicity involves both immediate and long-term heart-related toxic consequences (4). The precise mechanism underlying DOX-induced cardiotoxicity is still unknown, despite significant advancements in research methods and investigations throughout time. Numerous pathways are believed to be involved in DOX-induced cardiotoxicity, including oxidative stress, autophagy suppression, increased lipid peroxidation, DNA/RNA damage, endoplasmic reticulum-mediated apoptosis, and alteration of calcium homeostasis (5).

Cells' aerobic metabolic activity produces reactive oxygen species (ROS) such as superoxide which can cause oxidative stress as they upset the dynamic balance of cells (6,7). The imbalance between antioxidant defenses and ROS is the primary cause of oxidative stress, which is a significant contributor to a broad range of diseases. Small molecules such as vitamin E, vitamin C and glutathione and enzymes such as superoxide dismutase (SOD), catalase (CAT), and glutathione peroxidase (GSH-Px) serve as antioxidant defenses in living cells (6). If there are more oxidant species than antioxidants, redox equilibrium is disturbed, leading to oxidative stress and results in a variety of clinical disorders (8,9). Myocardial tissue is especially prone to free radical-induced damage because of the heart muscle's high metabolic rate and low antioxidant levels in comparison to other organs, which can cause irreversible damage to cardiac cells (10). Since oxidative stress is a major factor in the illness, many antioxidants have been investigated to counteract the cardiotoxicity of DOX (11). Autophagy serves two purposes by destroying defective proteins and organelles and preventing apoptosis, it either improves cellular function and survival or has the potential to cause cell death. So, the cellular environment and appropriate regulation of autophagy will depend on stressful stimuli (12). In pathological circumstances, elevated autophagy is detrimental in some cardiac disease states, such as cardiac hypertrophy, but protective in others, such as ischemia preconditioning (13). Recent research has looked at the involvement of autophagy in DOX-induced cardiotoxicity, although there are conflicting reports on how DOX affects autophagy and how it contributes to cardiotoxicity.

The cerium oxide nanoparticles (nanocerium or NC) have antioxidant and anti-inflammatory properties making it a promising antioxidant in a number of disorders (14,15). Also, it has been demonstrated that they act as free radical scavengers (16) 17). Researchers have shown that cerium oxide nanoparticles (NC) are far more powerful than cerium oxide (18). Because of these oxygen vacancies, NC is a potent antioxidant with potential for medical applications. Due to its redox regeneration capacity, NC might also be a noteworthy, rare earth-based nanoparticle for lowering oxidative stress-induced disorders. Additionally, by boosting levels of SOD and CAT and scavenging nitric oxide (NO) radicals by acting as their mimic, NC enhances its case against ROS-driven illnesses (15). Therefore, the favorable biological effects of NC that have been identified (such as reduction in oxidative stress and ROS scavenging) may guard against DOX-induced cardiotoxicity. We hypothesized that lowering oxidative stress by NC would be advantageous for preventing the DOX-induced cardiotoxicity. Therefore, the aim of the present work was to explain the relationship between autophagy as long as oxidative stress and the putative cardioprotective effects of NC against DOX-induced cardiotoxicity.

Materials and Methods

Animals

Forty-eight male Sprague-Dawley rats (weigh 250 ± 40 g, 4 months old) were housed in the

[DOI: 10.61186/rbmb.12.3.495]

medical experimental research center (MERC), Mansoura Faculty of Medicine. Rats were kept in a chamber with regulated humidity (65%), temperature (22 °C), and 12 hours of darkness and light. The rats were given free access to tap water and were given regular laboratory food. Our regional animal care and ethics committee approved all experimental protocols (code# MDP.20.12.53). All experimental protocols and procedures and the animal care guidelines followed the Guide for the Care and Use of Laboratory Animals.

Experimental design

After one week of acclimatization period, rats were divided into four groups (8 rats each) as follow; i) control group; were normal rat fed on standard chow for 8 weeks, ii) NC group; were normal rats which received 0.2 mg/kg cerium oxide nanoparticle (NC) daily intraperitoneally, (14), iii) DOX group: were rats injected with 2 doses of DOX at a 14-day interval, each dose (4 mg/kg) in 0.5 ml saline via penile vein for 8 weeks without NC (19), and iv) DOX+NC group; were rats injected I.P by 0.2 mg/kg NC daily 2 hrs prior to DOX injection (14).

The electrocardiogram (ECG) recording

Biopac's student lab system (software BSL 3.7.6, USA), data acquisition unit MP36, Biopac electrode lead set x 2, and disposable vinyl electrodes, 3 electrodes per rat, were used to record the ECG on rats in each group that had been given xylazine (16 mg/kg i.p.) and ketamine (80 mg/kg i.p.). QRS complex, P-R interval, QT intervals, corrected QT (QTc) intervals, heart rate (HR), ST segments were calculated from different ECG records in each group.

Echocardiographic Examination

At the end of the study, under controlled anesthesia with ketamine (80 mg/kg i.p.) and xylazine (16 mg/kg i.p.), echocardiography was done. Echocardiography was done using with a S8-3 probe with 2- dimension (D) M-mode echocardiograph (Philips, MATRIX, EPIC 7C, Model IE33, Germany). All measures were performed using the best digital images that the sonographer had chosen from at least 10 cardiac cycles. At the tips of the papillary muscles, the diameters of the ventricles (LV), the thickness of the interventricular septum, and the posterior wall were measured. In a single-plane, four-chamber view, the LV end-systolic and end-diastolic regions were traced, and the ejection % was computed. Analysis of at least 10 distinct cardiac cycles. For evaluation of the myocardial contractility the fractional shortening (FS) (%) and ejection fraction (EF) (%) were calculated. While, left ventricular internal diameter end diastole (LVIDd) and left ventricular internal diameter end systole (LVIDs) were calculated to evaluate the left ventricular dimensions and hypertrophy.

Collection of blood samples and harvesting the heart

Blood samples were collected via cardiac puncture under sodium thiopental (120 mg/Kg) inhalation anesthesia, then the thorax was opened, and the heart tissue was quickly removed. Blood samples were centrifuged, and sera were collected and stored at -20 °C for measurement of cardiac enzymes; CK-MB and LDH. The heart was then cleaned with isotonic ice-cold saline and divided into two parts. The small part of the heart was used for measuring oxidative stress markers, electron microscopic analysis, and molecular studies, while the larger portion of the heart was soaked in 10% neutral formalin for histopathological and immunostaining studies.

Biochemical assay

Assay of cardiac enzymes (LDH and CK-MB)

According to the manufacturer's, instructions, lactate dehydrogenase (LDH) (Human-Company, Egypt) and creatine kinase-MB (CK-MB) (Cloud Clone company, USA) were measured using commercially accessible kits (Bio-Diagnostics, Giza, Egypt).

Assay of myocardial oxidant/ antioxidant biomarkers

About 100 mg of the cardiac tissues were homogenized in cold phosphate buffer saline (pH 7.4, 50 mM). Malondialdehyde (MDA), catalase enzyme (CAT) and reduced

[DOI: 10.61186/rbmb.12.3.495]

glutathione (GSH) were measured in tissue homogenate by colorimetric kits (Bio-Diagnostics, Giza, Egypt) following the manufacturer's instructions.

Quantitative real time PCR

The mRNAs encoding for metabolic marker (acetyl-CoA carboxylase alpha, ACACA) in heart tissues were obtained from Vivantis Technologies Company, Malaysia. According to the manufacturer's instructions, we isolated the total RNA from heart tissue specimens. RNA was quantified spectrophotometrically, and its quality was determined by agarose gel electrophoresis and ethidium bromide staining. cDNA was synthesized from 1 µg total RNA and then buffered in a volume of 25 µL. All steps of PCR reaction and calculation of the gene expression were mentioned in a previous study (20). The primer sequences of the tested (ACACA) and housekeeping (GAPDH) genes are listed in Table 1.

Table 1. Primer sequence of the examined genes.

Gene		Forward sequence (5'–3')	Size (bp)	GenBank Accession No.
ACACA	**Forward**	5'-ATATGTTCGAAGAGCTTATATCGCCTAT-3'	7038	NM_022193.1
	Reverse	5'-TGGGCAGCATGAACTGAAATT-3'		
GAPDH	**Forward**	5'-AGACAGCCGCATCTTCTTGT-3'	1306	NM_017008.4
	Reverse	5'-TTCCCATTCTCAGCCTTGAC -3'		

Assay of AMPK by ELISA

The level of 5' adenosine monophosphate-activated protein kinase (AMPK), a metabolic marker, was measured in myocardial homogenates via AMPK ELISA kits for rat that purchased from the company of R&D system, Inc. USA & Canada #cat no. DYC3197-5.

Histopathological examination

The gathered cardiac tissues were then preserved in 10% buffered neutral formalin solution after being rinsed with saline. The cardiac tissue was handled and embedded in paraffin after fixing. The heart tissues were then divided into sections and stained with hematoxylin and eosin (H&E). The heart specimens were examined for loss of myocardial striations, myocardial cell necrosis, and inflammatory cell infiltrates.

Immunohistopathological examination for caspase-3, Beclin-1 and LC3

The tissue sections were incubated with antibodies against LC3 rabbit polyclonal (1:1200; catalog no. GB13431); active Caspase-3 rabbit polyclonal (1:1000; catalog no. GB11532, Service bio); and Beclin1 rabbit polyclonal (1: 4000; catalog no. GB11228). Then, they were incubated with UltraVision One HRP Polymer for 15 minutes. Then, Substrate/Chromogen Solution (Reagent B1) was ready to be used and mixed with DAB Buffer Solution (Reagent B2) in a 1:1 ratio with the volume that is defined by the quantity of stained slides. In general, one tissue slide might be covered with 200 uL of mixed substrate solution. Using image J software, the expression of caspase-3, Beclin-1, and LC3 was measured as the percentage of myocardial area occupied by positive staining for each left ventricular area (determined by averaging the values from ten fields at 10 magnification).

Transmission Electron Microscopy (TEM)

Fine fragments (1x1x1mm) were rapidly fixed in mixed paraformaldehyde (4%) /glutaraldehyde (1%) (4F1G) fixative solution. Then, the specimens were dehydrated and embedded in epoxy resins. Toluidine blue was used to stain semithin slices (1 um thickness). Uranyl acetate and lead citrate were used to stain ultrathin slices (60-70 nm thickness). Electron microscopic examination was done at the faculty of Agriculture, Mansoura University. It was performed using (JEOL JEM-2100, Japan) transmission electron microscope at 200 KV.

[DOI: 10.61186/rbmb.12.3.495]

Statistical analysis

Data were presented as mean± SD. Analysis of variance (ANOVA) was used to compare parametric data, and Tukey's post hoc analysis was used to compare data among groups. P< 0.05 is considered significant.

Results

Effects of cerium oxide nanoparticles (NC) on ECG parameters and echocardiographic parameters

The ECG parameters PR interval, QT interval, QRS duration and amplitude, ST segment showed no statistically significant difference among all studied groups. While HR in DOX, group showed significant decrease compared to the control and NC groups (P< 0.001). Moreover, the DOX+NC group showed more significant improvement in HR when compared to the DOX group only (P< 0.01). Regarding the QTc interval, the DOX group showed a significant increase when compared with the control group (P< 0.05) with a non-significant change in comparison with NC group. Also, DOX+NC group showed a non-significant change if compared with the DOX group (Table 2 and Fig. 1).

Also, the echocardiographic parameters; LVIDs and LVIDd showed no statistically significant difference among all studied groups. On the other hand, FS% and EF% showed significant reduction in DOX group compared to the control and NC groups (P< 0.01 and P< 0.01, respectively). On the other hand, FS% and EF % showed significant rise in DOX+NC group compared to DOX group (P< 0.05) (Table 2).

Table 2. Effects of cerium oxide nanoparticles (NC) on ECG parameters and echocardiographic parameters in DOX-induced cardiomyopathy.

		Control group (N=8)	NC group (N= 8)	DOX group (N=8)	DOX+NC group (N=8)
ECG parameters	**P-R interval (sec)**	0.045±0.008	0.0402±0.0055	0.036±0.008	0.045±0.013
	QRS duration (sec)	0.036±0.002	0.034 ±0.0037	0.033±0.0015	0.035±0.0038
	QRS amplitude (mv)	0.415±0.01	0.35±0.044	0.35±0.08	0.36±0.029
	QT interval (sec)	0.093±0.015	0.10 ±0.008	0.11±0.02	0.12±0.02
	QTc (sec)	0.178±0.03	0.21 ±0.016	0.22±0.03*	0.23±0.023
	ST segment (mV)	-0.05±0.04	0.0245±0.002	-0.038±0.04	-0.039±0.003
	HR (bpm)	254.0 ± 6.0	249.67 ± 24.7	187±7.7$^{*, \#}$	263.5 ±42.03$^{\$}$
	R-R (sec)	0.27±0.013	0.238 ± 0.027	0.27±0.05	0.24 ± 0.046
Echocardiographic parameters	**LVIDs (mm)**	3.4±0.5	3.23± 0.25	4.16±1.24	3.98 ± 0.55
	LVIDd (mm)	5.8±0.76	5.67±0.51	5.7±1.6$^{\#}$	6.0 ± 0.89
	EF%	75±12.7	83.33 ± 4.93	64.8±5.0$^{*, \#}$	80.17 ± 5.56$^{\$}$
	FS%	46.7±3.4	47.0 ± 4.73	30.8±3.7$^{*, \#}$	48.0±3.38 $^{\$}$

All results are expressed as mean ± SD, One-way ANOVA with Tukey post hoc test (significance at P≤ 0.05), *significant vs control group, # significant vs NC group, $ significant vs DOX group. NC= Nanocerium, DOX= doxorubicin, HR= heart rate, LVIDd= left ventricular internal diameter end diastole, LVIDs= left ventricular internal diameter end systole, FS= fractional shortening and EF = ejection fraction. DOX= doxorubicin.

[DOI: 10.61186/rbmb.12.3.495]

Fig. 1. ECG traces recorded from a) control group, b) nanocerium (NC) group, d) Doxorubicin (DOX) group, and d) DOX+NC group.

Effects of cerium oxide nanoparticles (NC) on cardiac enzymes (CK-MB, LDH) and myocardial oxidative stress markers (MDA and CAT and GSH)

Serum levels of cardiac enzymes (CK-MB, and LDH) showed significant rise in DOX group compared to control and NC groups ($P< 0.05$). Also, the DOX+NC group showed significant decrease in both cardiac enzymes compared to DOX group ($P< 0.05$) (Table 3). Also, DOX group showed significant increase in MDA ($P< 0.001$) compared to control and NC groups with significant decrease in the GSH concentration and CAT activity ($P< 0.01$) compared to control and NC groups in the heart tissues. On the other hand, DOX+ NC group showed a significant decrease in the concentration of MDA ($P< 0.01$), with significant increase in GSH expression ($P< 0.05$) and catalase activity ($P< 0.01$) compared to DOX group.

Table 3. Effects of cerium oxide nanoparticles (NC) on cardiac enzymes (CKMB and LDH) and myocardial oxidative stress markers (MDA, GSH and catalase activity) in DOX-induced cardiomyopathy.

Group	Control (N=8)	NC (N=8)	DOX (N=8)	DOX + NC (N=8)
Serum CKMB (U/L)	666.5±119. 9	505.85 ± 139.71	1341.4±405.7$^{*,\#}$	791.89 ± 281.94$^{\$}$
Serum LDH (mg/dl)	1154.87±260.25	681.00 ± 138.31	2212.17±646.7$^{*,\#}$	1466.53 ± 550.89$^{\$}$
MDA (nmol/mg protein)	584.43 ±177.25	409.10 ± 69.72	1571.38±303.75$^{*,\#}$	478.80 ± 113.65$^{\$}$
Reduced glutathione (GSH) (nmol/mg protein)	11.54 ± 4.13	5.319 ± 0.29**	7.54 ± 3.0*	11.11 ± 5.36$^{\$}$
Catalase (unit /mg protein)	1321.08 ± 454.4	1227.97 ± 308.43	249.98±55$^{*,\#}$	1235.38±337.02$^{\$}$

All results are expressed as mean ± SD, One-way ANOVA with Tukey post hoc test (significance at $P\leq 0.05$), *significant vs control group, # significant vs NC group, $ significant vs DOX group. DOX= doxorubicin, NC= Nanocerium, MDA= malonaldehyde.

[DOI: 10.61186/rbmb.12.3.495]

Effects of cerium oxide nanoparticles (NC) on myocardial metabolic biomarkers (ACACA and AMPK)

The DOX group showed a significant increase in the ACACA gene expression compared to control and NC groups (P< 0.01). Moreover, the DOX+NC group showed a significant decrease (P< 0.05) compared to DOX group (Fig. 2A). Compared to the control group, the NC group showed significant increase in the AMPK myocardial level (P≤ 0.01). Moreover, the DOX group showed a significant decrease (P≤ 0.0001) in comparison with NC group and a non-significant change with control group. The DOX+NC significantly increased expression of AMPK (P≤ 0.01) compared to the DOX group (Fig. 2B).

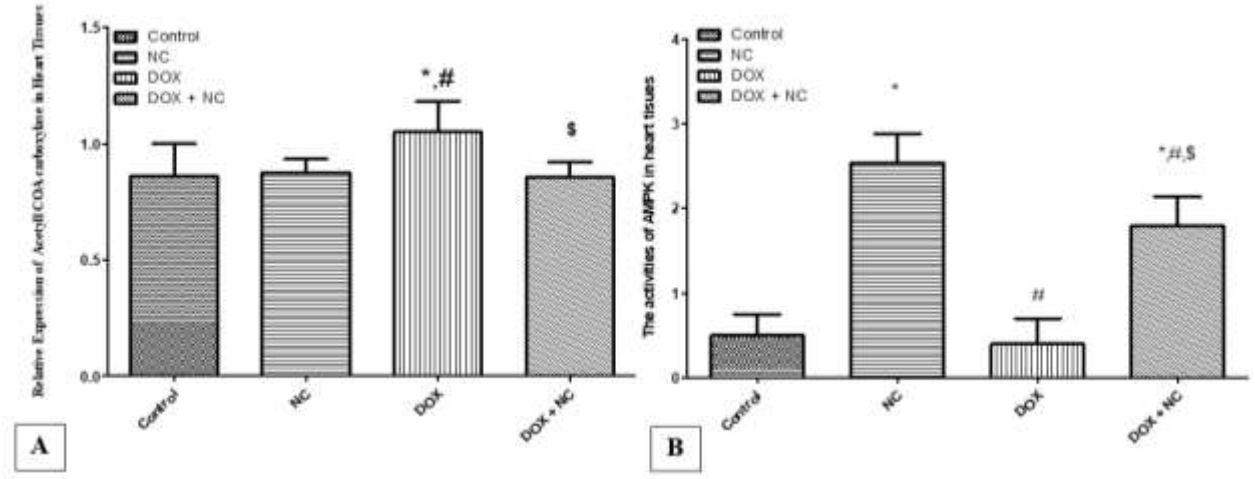

Fig. 2. Effects of cerium oxide nanoparticles (NC) on the levels of metabolic markers; including A) Acetyl-CoA carboxylase alpha, (ACACA) expression at the level of mRNA by real time PCR and (B) 5'adenosine monophosphate-activated protein kinase (AMPK) by ELISA in heart tissue in different groups. *Significant vs control group, # significant vs NC group, $ significant vs DOX group.

Effects of cerium oxide nanoparticles (NC) on myocardial morphology:

The heart specimens from control and NC groups showed regularity of cell and nuclear membrane and normal architecture of the myocardium (Figs. 3 A and B), while those from DOX group showed disarrangement and degeneration of the myocardium, loss of normal myofibril striation with patches of necrotic and apoptotic areas (Fig. 3C). On the other hand, the heart specimens from DOX+NC showed nearly normal cellular pattern and striation with mild interstitial edema (Fig. 3D).

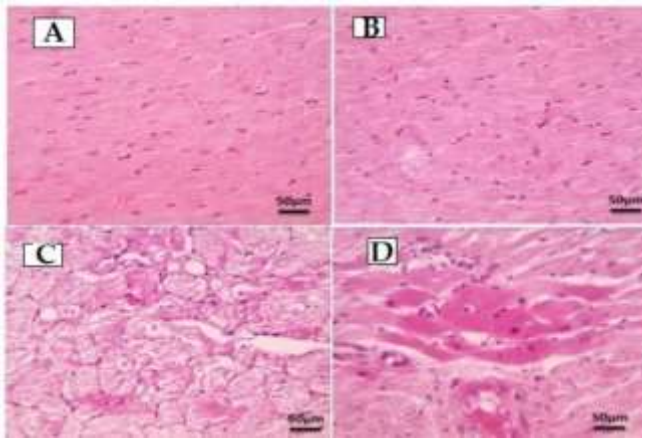

Fig. 3. Photomicrographs of heart specimens from different groups. The heart specimens from A) control group show normal arrangement of cardiac muscle fibres with regularity of cell and nuclear membrane, B) NC group show normal arrangement of cardiac muscle fibres, regularity of cell and nuclear membrane, normal nuclear pattern of cells, C) DOX group show disarrangement and degeneration of the myocardium, loss of normal myofibril striation, necrotic and apoptotic areas and D) DOX +NC group show return of the myocardial morphology to normal cellular pattern and striation, little cellular infiltration and mild interstitial edema (H & E, 400x).

[DOI: 10.61186/rbmb.12.3.495]

Effects of cerium oxide nanoparticles (NC) on the ultrastructure of the myocardium

Electron microscope micrographs from control and NC groups show normal structure of myofibrillar striations, shape of sarcomere, shape and size of mitochondria, chain with prominent euchromatic oval nucleus with distinct nucleolus (Figs. 4A and B), while the ultrastructure of DOX group showed massive fragmentation, loss of normal striation with myofibrillar loss with interrupted Z line and intercalated disk, irregular shape of scattered degenerated mitochondria with less densely chromatic oval nucleus and multiple rounded vesicles referred to autophagosomes (Fig. 4C). On the other hand, DOX+NC group showed mild myofibrillar loss and spaces with normal Z lines and intercalated disks, normal structure of mitochondria with less densely chromatic oval nucleus and multiple rounded vesicles referred to autophagosomes (Fig. 4D).

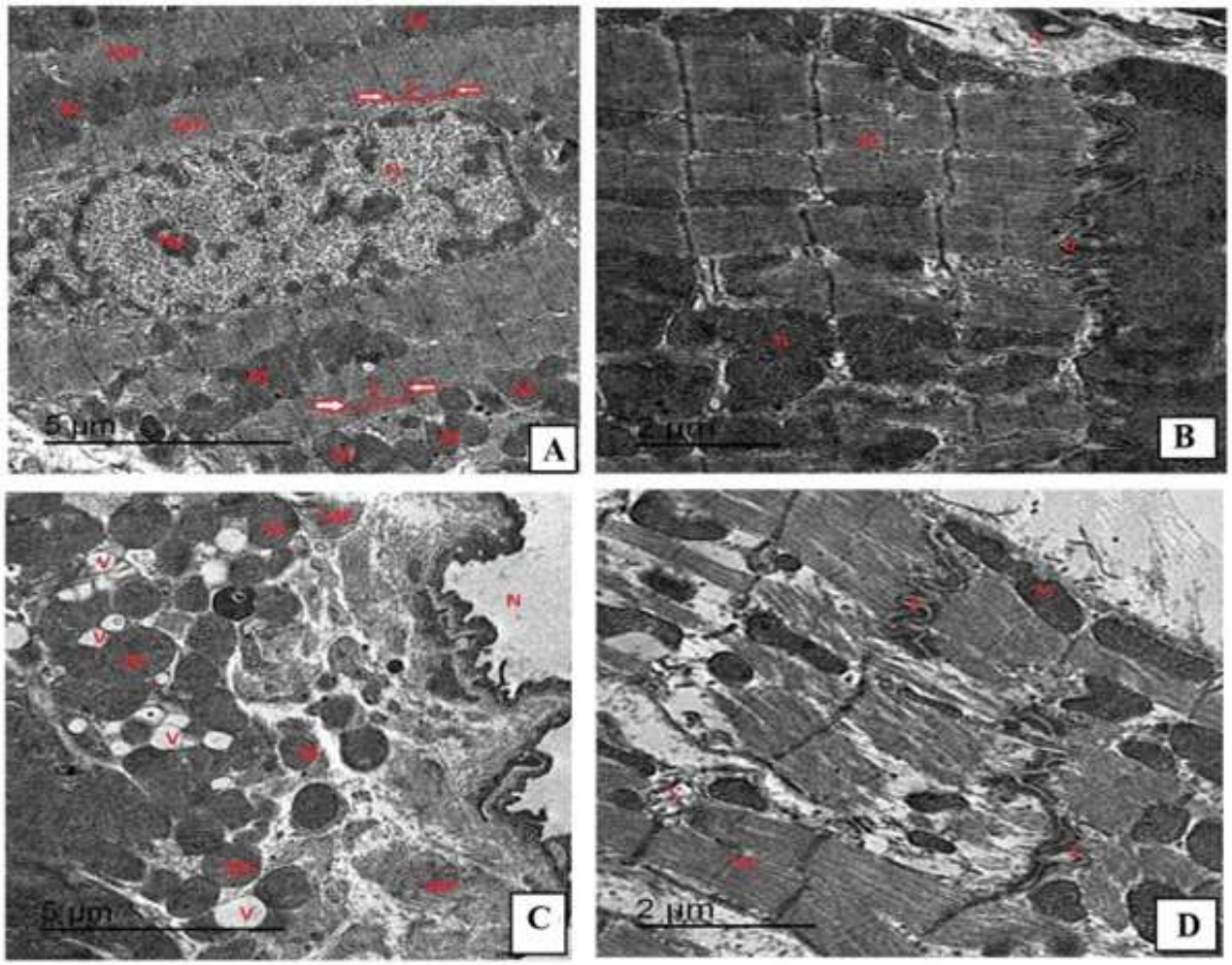

Fig. 4. Photomicrographs of the heart tissues by electron microscope from A) control group show normal structure of myofibrillar striation and arrangement (MF) with normal shape of sarcomere (S, RT and LT directed arrow referred to Z line), normal shape of mitochondria (M) large, rounded, chain with prominent euchromatic oval nucleus (N) with distinct nucleolus (Nu), B) NC group show normal structure of myofibrillar striation and arrangement (MF) with normal shape of sarcomere (S, RT and LT directed arrow referred to Z line) which separated by normal intercalated disk (D), normal shape of mitochondria (M) large, rounded, chain. with prominent euchromatic oval nucleus (N) with distinct nucleolus (Nu) with multiple rounded vesicles referred to autophagosomes, C) DOX group show massive fragmentation, loss of normal striation with myofibrillar loss (MF) with interrupted Z line (RT and LT directed arrow referred to Z line) and intercalated disk (D), irregular shape of scattered degenerated mitochondria (M) with less densely chromatic oval nucleus (N) and multiple rounded vesicles referred to autophagosomes, and D) DOX+NC group show moderate changes as partial loss of architecture with preservation of normal striation with less myofibrillar loss and spaces (MF) with normal Z line (RT and LT directed arrow referred to Z line) and intercalated disk (D), retained normal structure of mitochondria (M), less densely chromatic oval nucleus (N) with multiple rounded vesicles referred to autophagosomes.

[DOI: 10.61186/rbmb.12.3.495]

Effects of cerium oxide nanoparticles (NC) on the expression of caspase-3, LC3 and Beclin-1 in myocardial tissues

Measuring the level of caspase-3 expression of by immunostaining revealed significant increase in its expression in DOX group compared to control and NC groups (P< 0.001). Besides, its expression was significantly reduced in DOX+NC group compared to DOX group (P< 0.01) (Fig. 5A). Hearts tissues with minimal cytoplasmic expression of caspase-3 in cardiomyocytes from control and NC groups were found respectively (Figs. 5B and C). However, the DOX group heart specimens showed marked cytoplasmic expression of caspase-3 in myocardial tissues (Fig. 5D), while hearts obtained from DOX+NC group showed mild cytoplasmic expression of caspase-3 in cardiomyocytes (Fig. 5E).

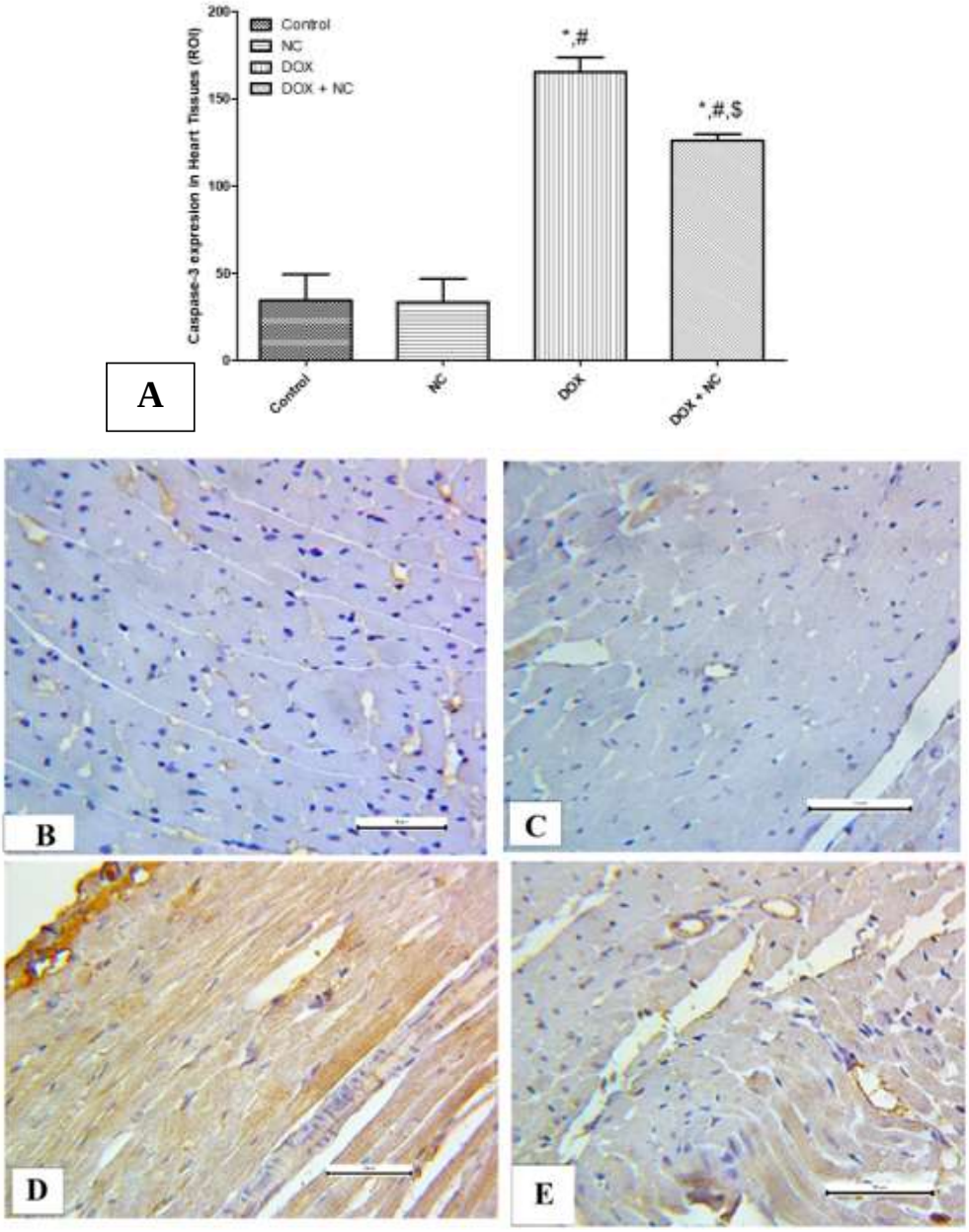

Fig. 5. Effects of cerium oxide nanoparticles (NC) on the expression of caspase-3 in DOX-induced cardiomyopathy. The means area of expression of caspase-3 in the heart tissues of different studied groups (A). Photomicrographs of the myocardium showing B= minimal caspase-3 expression (control group), C= minimal caspase-3 expression (NC group), D= marked expression of caspase-3 (DOX group) and E = minimal expression of caspase-3 (DOX + NC). *Significant vs control group, # significant vs NC group, $ significant vs DOX group.

[DOI: 10.61186/rbmb.12.3.495]

Measuring the level of beclin-1 expression by immunostaining revealed that DOX group caused a significant increase in beclin-1 expression if compared to control and NC groups ($P \leq 0.05$). In addition, its expression was significantly reduced in DOX+NC group compared to DOX group ($P < 0.001$) (Fig. 6A). Hearts tissues with minimal cytoplasmic expression of beclin-1 in cardiomyocytes from control, and NC groups were found (Figs. 6 B and C respectively). However, the DOX group heart specimens showed marked cytoplasmic expression of beclin-1 in myocardial tissues (Fig. 6D), while hearts obtained from DOX+NC groups showed mild cytoplasmic expression of beclin-1 in cardiomyocytes (Fig. 6E).

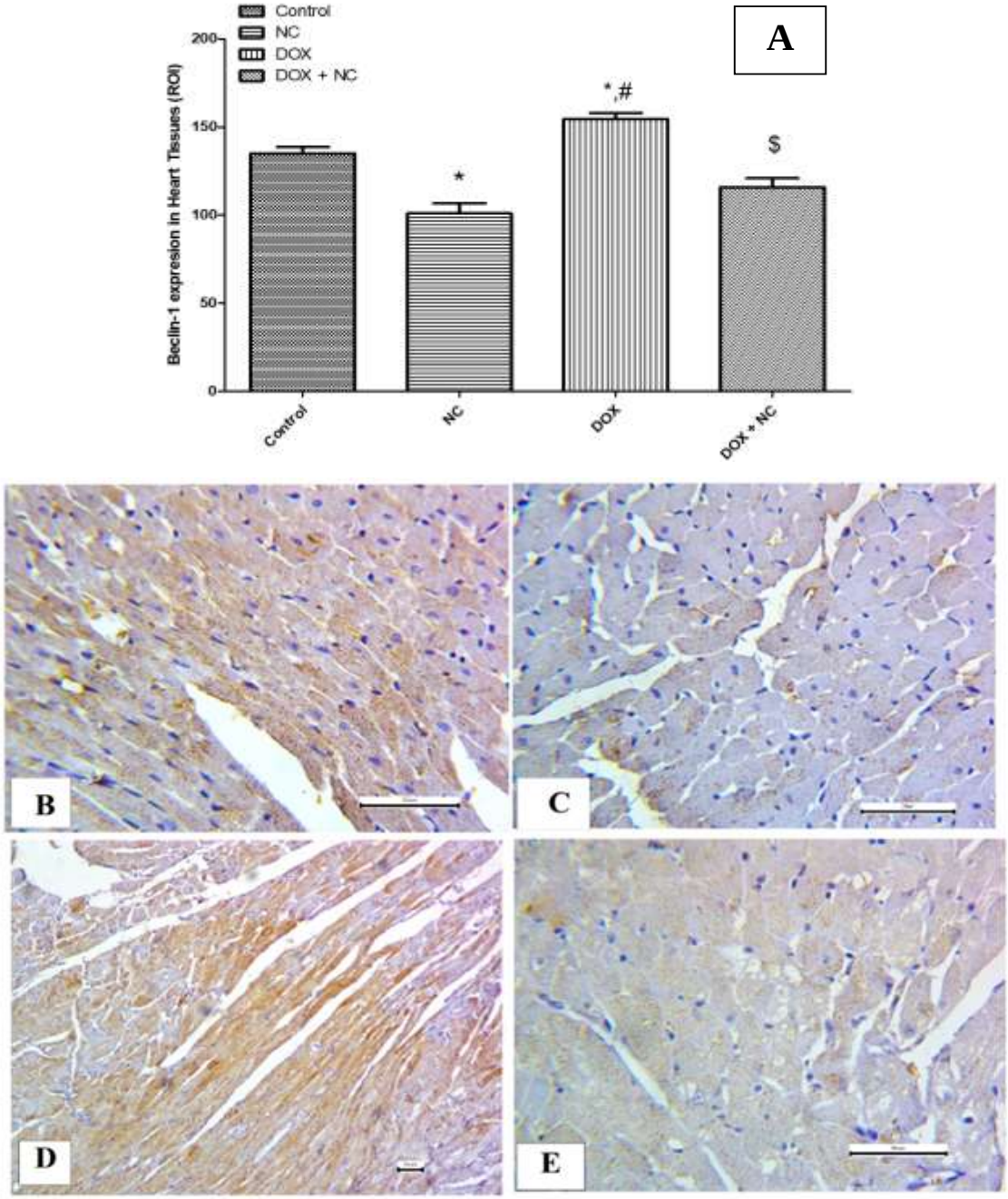

Fig. 6. Effects of cerium oxide nanoparticles (NC) on the expression of Beclin-1 in DOX-induced cardiomyopathy. The means area of expression of Beclin-1 in the heart tissues of different studied groups (A). Photomicrographs of the myocardium showing B= minimal Beclin-1 expression (control group), C= minimal Beclin-1 expression (NC group), D= marked expression of Beclin-1 (DOX group) and E = minimal expression of beclin-1 (DOX+NC group). *Significant vs control group, # significant vs NC group, $ significant vs DOX group.

[DOI: 10.61186/rbmb.12.3.495]

Measuring the level of LC3 expression by immunostaining revealed a significant increase in DOX group compared to control and NC groups (P< 0. 001). In addition, its expression was significantly attenuated in and DOX+NC group compared to DOX group (P< 0.001) (Fig. 7A). Hearts tissues with minimal cytoplasmic expression of LC3 in cardiomyocytes from control, and NC groups were found, respectively (Figs. 7B and C). However, the DOX group heart specimens showed marked cytoplasmic expression of LC3 in myocardial tissues (Fig. 7D), while hearts obtained from DOX+NC groups showed mild cytoplasmic expression of LC3 in cardiomyocytes (Fig. 7E).

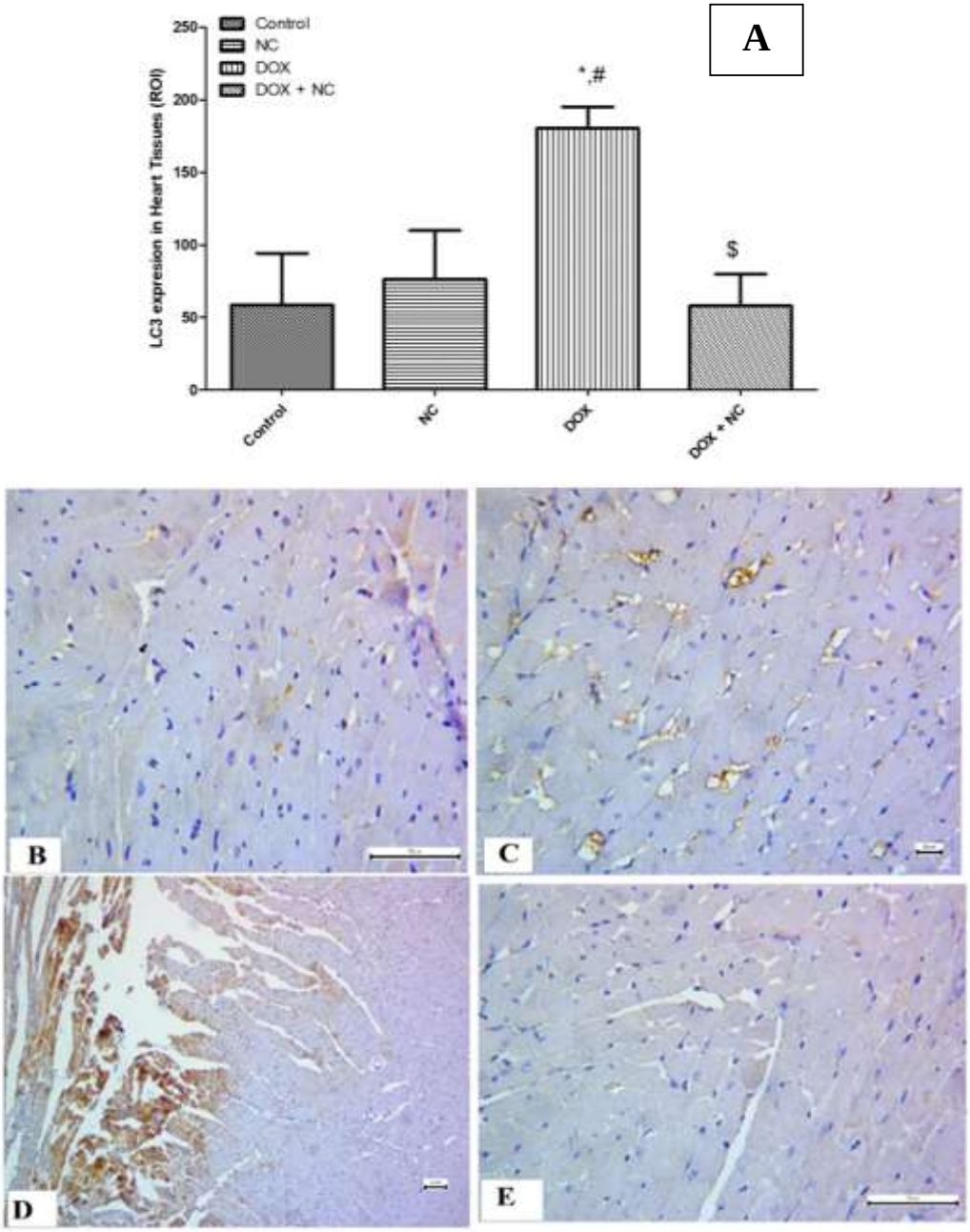

Fig. 7. Effects of cerium oxide nanoparticles (NC) on the expression of LC3 in DOX-induced cardiomyopathy. The means area of expression of LC3 in the heart tissues of different studied groups (A). Photomicrographs of the myocardium showing B= minimal LC3 expression (control group), C= minimal LC3 expression (NC group), D= marked expression of LC3 (DOX group) and E = minimal expression of LC3 (DOX+NC group). *Significant vs control group, # significant vs NC group, $ significant vs DOX group.

[DOI: 10.61186/rbmb.12.3.495]

Discussion

The main findings of the current work can be summarized as follow; i) administration of DOX caused a significant decline in cardiac functions (as shown from the results of cardiac enzymes LDH and CK-MB, ECG recording and echocardiography), cardiac morphology, and induction of autophagy and ii) use of cerium oxide nanoparticles (NC) significantly improved the myocardium's altered structures and functions as well as its metabolic dysfunctions. In line with previous studies, injection of DOX at a 14-day interval, each dose measured 4 mg/Kg twice caused significant rise in both cardiac enzymes LDH and CK-MB confirming the development of impairment of the cardiac functions **(**21**)**. By significantly lowering shortening fraction (SF) percentage % and ejection fraction (EF) in the DOX group utilizing echocardiography, the current study's impairment of cardiac functions with DOX treatment was further supported. These results are consistent with earlier research that documented by Wang et al., **(**22**)**. Podyacheva et al., (23) indicated a more than 10% drop in EF because of cardiomyocyte injury. The corrected QT (QTc) interval was longer on the ECG, and the heart rate (HR) was lower in the DOX group. These are consistent with those reported by Warhol and his colleagues **(**24**)**.

Also, the current study showed several histopathologic alterations in cardiac muscles. These lesions showed a sarcoplasmic alteration, muscle fiber dissociation, and striation loss in addition to a modification of the usual architecture. We noticed necrotic and apoptotic regions on the slices. Additionally, in one case, areas of inflammation were seen in conjunction with a lymphoid infiltrate **(**25**)**. Perinuclear vacuolation, pronounced interstitial edema, interfibrillar bleeding, inflammatory cellular infiltration surrounding blood vessels, strongly eosinophilic cytoplasm, myocardial disarray, and degeneration **(**26**)**. It has been demonstrated that doxorubicin induces apoptosis in cell culture models, isolated myocytes, and the heart of rats **(**25**)**. Electron microscopic analysis of the heart reveals that DOX causes cardiomyocyte cytoplasmic vacuolization and myofibril degeneration and/or loss. In addition, ultrastructural examination reveals loss of plasmalemmal integrity and the presence of damaged mitochondria. Moreover, there was vacuoles forming large membrane-bound spaces as confirmed by Agaba et al., (27) and Ivanová et al., **(**28**)**.

On the other hand, pretreatment with cerium oxide nanoparticles (NC) was found to diminish the toxicity of DOX on heart tissue. NC returned the levels of cardiac injury markers as LDH and CK-MB to normal levels. Moreover, NC reduced MDA oxidant marker levels and increased endogenous antioxidants such as GSH and catalase levels in line with Sangomla et al., (14) and Kumari et al., **(**15**)** as well as echocardiographic parameters including FS% and EF and ECG parameters including QTc interval. Our results agree with those reported by Niu et al., **(**29**)** and Kumari et al., **(**15**)** who illustrated protective role of NC on echocardiographic parameters in rat model of cardiomyopathy and ECG parameters in rat model of cardiac remodeling. Also, the histopathological and structural examination of the myocardium by electron microscope revealed preserved myocardium morphology and ultrastructure in rats treated with NC in DOX-induced cardiomyopathy which suggest the cardioprotective effect of NC.

Although the exact mechanism of DOX-induced cardiotoxicity is unclear until now, it has been demonstrated that oxidative stress, mitochondrial malfunction, and apoptosis may play a role **(**30**)**. Increased autophagosome accumulation, abnormal expression of oxidative respiration regulatory proteins and mitochondrial dynamics that impaired mitochondrial respiration were all seen in the DOX cardiomyopathy model **(**31**)**. Oxidative stress that is caused by reactive oxygen species (ROS), is considered a critical stage in the onset and development of DOX-induced cardiomyopathy. At first, it was postulated that doxorubicin's direct contact with the transport chain of mitochondrial electron would result in the production of early ROS. The cardiac

[DOI: 10.61186/rbmb.12.3.495]

tissue has lower levels of enzymatic antioxidant defenses if compared to liver and kidney, which can make the heart more vulnerable to free radical damage **(**32**)**. Uncoupled nitric oxide synthase (NOS), mitochondria, and nicotinamide adenine dinucleotide phosphate (NADPH) oxidases (NOX) are all regarded as pertinent sources of ROS that contribute to the development of vascular and cardiac dysfunction at the level of cardiac cells. By triggering hypertrophic signaling, apoptosis, necrosis, and autophagy, ROS controls myocardial calcium (Ca^{2+}) overload, an occurrence that contributes to contractile failure, arrhythmias, and the maladaptive cardiac remodeling process **(**32**)**. Targeting topoisomerase II- and producing reactive oxygen species as a result of mitochondrial iron buildup are two of the many ways that DOX causes cardiomyocyte death **(**33**)**. In the current study development of oxidative stress in cardiac tissues by DOX is evidenced by significant elevation in MDA with significant reduction in the antioxidants GSH and catalase in DOX group. Moreover, administration of NC with DOX significantly attenuated the oxidative stress suggesting that NC might have protective antioxidant effect against DOX-induced cardiomyopathy.

Despite these advancements in knowledge, there is currently little information on the antioxidant and anti-apoptotic effects of NC on DOX cardiotoxicity. Pretreatment of DOX induced cardiomyopathy via NC resulted in significant elevation in expression levels of caspase 3, an effector caspase, which mediate the terminal stages of apoptosis process in heart tissue. On the other hand, NC significantly reduced the expression of caspase-3 in heart tissues suggesting anti-apoptotic action for NC in DOX-induced cardiomyopathy. It has been demonstrated that NC could scavenge free radicals i.e., acts as direct antioxidant and reducing cell death induced by oxidative stress **(**34**)**. Therefore, NC have been found to possess significant capabilities in tissue repair and regenerative medicine based on their antioxidant and antiapoptotic properties.

Several studies investigated the potential role of autophagy in the genesis and progression of DOX-induced cardiomyopathy showed mixed results **(**35**)**. Both in vitro and in vivo analyses showed that DOX-cardiotoxicity results in either increased **(**36-38**)** or decreased **(**39,40**)** autophagy activity. To verify these conflicts, we used immunohistopathology staining for beclin1 and LC3 (autophagy markers) to investigate the DOX-mediated change at various autophagic phases. In our research, the DOX-cardiomyopathy model demonstrated a slow buildup of autophagosomes as a result of a malfunction in the autophagic degradation mechanism. Previous studies showed that the chronic DOX therapy inhibits the autophagic flux of cardiomyocytes both in vivo and in culture, and this is followed by a significant buildup of autolysosomes that have not yet destroyed **(**40**)**. However, the immunohistopathology results of LC3 and Beclin 1 which indicated the accumulation of autophagosomes, were attenuated in NC-treated cardiac tissues. In agreement with these findings, the results of electron microscope (EM) in the current study found that the number of autophagosomes in NC+DOX groups were similar to that in control and NC control group. These outcomes explained that NC exposure could activate and regulate the whole autophagy process in cardiac tissue are in line with Chen et al. **(**41**)**.

In the present study, we assessed the ability of the NC in modulating mitochondrial functions and bioenergetics by evaluating the activity of 5’adenosine monophosphate-activated protein kinase (AMPK) and the expression of acetyl-CoA carboxylase alpha (ACACA) at the mRNA levels. AMPK, a key regulator of autophagy, is a member of a conserved family of protein kinases that is activated by ATP depletion e.g. during cellular starvation and results in AMP buildup **(**42**)**. It has been demonstrated that AMPK activation decreases the intracellular malonyl CoA concentrations by inhibiting ACACA (rate-limiting enzyme of malonyl CoA synthesis) and stimulating malonyl CoA decarboxylase (MCD) (rate limiting enzyme of malonyl CoA

[DOI: 10.61186/rbmb.12.3.495]

degradation), so stimulates the fatty acid oxidation in the heart tissues **(**39,43**).** In the current study, we found that DOX greatly lowered the activity of AMPK with upregulation of ACACA enzyme suggesting impairment of the fatty acid oxidation in the cardiac tissues by DOX toxicity. On the other hand, NC treatment restores the activity of AMPK and ACACA levels in the myocardium suggesting improvement of the metabolic activity in the heart tissues by NC therapy. Thus, the mitochondrial benefits from the restoration of AMPK activation, which lowers oxidative stress and maintains mitochondrial energy generation might be a possible mechanism for the cardioprotective effect of NC against DOX-induced cardiomyopathy **(**44**)**. Moreover, one of the cardiac targets of AMPK is mTOR signaling molecule, that regulates protein synthesis, autophagy and cardiac metabolism **(**45**)**. Kawaguchi et al., (42) found that DOX suppression of AMPK was the cause of its inhibitory effect on autophagy.

It is doubtful if NC would be a realistic cardioprotective strategy for cancer patients given that they already experience symptoms from their underlying illness and the side effects of treatment. They are yet regarded as preliminary results that require additional research to elucidate the impact of DOX on the autophagy process as p62 protein (a selective autophagy receptor) and markers of fibrogenesis. This issue is seen as a limitation of the current study.

In conclusion, NC may preserve the cardiac functions and structure in DOX-induced cardiomyopathy. This effect could be due to suppression of myocardial oxidative stress and apoptosis as well as autophagy regulation (via downregulation of Beclin-1 and LC3). Activation of AMPK might play an important role in autophagy regulation in cardiac muscle.

Funding

This work was funded by Mansoura university Research unit # Mu-Med-21-33.

Institutional Review Board Statement

All experimental protocols and procedures and the animal care guidelines followed the Guide for the Care and Use of Laboratory Animals and approved from the IRB, Mansoura Faculty of medicine (code # MDP.20.12.53).
This is experimental animal not human study which was approved by our local ethical committee.

Acknowledgments

Authors acknowledge the technicians and Veterinarians in the medical experimental research center (MERC), Mansoura Faculty of Medicine, for helping us in collection of blood samples and tissues from the animals.

Conflicts of Interest

All authors declared that there was no conflict of interest in this study.

References

1. Jarvis S. Electrocardiogram 1: purpose, physiology and practicalities. Nurs Times. 2021;117(6):22-6.
2. McKenna WJ, Maron BJ, Thiene G. Classification, Epidemiology, and Global Burden of Cardiomyopathies. Circ Res. 2017;121(7):722-730.
3. Carvalho FS, Burgeiro A, Garcia R, Moreno AJ, Carvalho RA, Oliveira PJ. Doxorubicin-induced cardiotoxicity: from bioenergetic failure and cell death to cardiomyopathy. Med Res Rev. 2014;34(1):106-35.
4. Mobaraki M, Faraji A, Zare M, Dolati P, Ataei M, Manshadi HRD. Molecular Mechanisms of Cardiotoxicity: A Review on Major Side-effect of Doxorubicin.Indian J Pharm Sci. 2017;79(3):335-44.
5. Songbo M, Lang H, Xinyong C, Bin X, Ping Z, Liang S. Oxidative stress injury in doxorubicin-induced cardiotoxicity. Toxicol Lett. 2019;307:41-48.
6. Finkel T, Holbrook NJ. Oxidants, oxidative stress and the biology of ageing. Nature. 2000;408(6809):239-47.

[DOI: 10.61186/rbmb.12.3.495]

7. Juan CA, Pérez de la Lastra JM, Plou FJ, Pérez-Lebeña E. The Chemistry of Reactive Oxygen Species (ROS) Revisited: Outlining Their Role in Biological Macromolecules (DNA, Lipids and Proteins) and Induced Pathologies. Int J Mol Sci. 2021;22(9):4642.
8. Kaneto H, Katakami N, Matsuhisa M, Matsuoka TA. Role of reactive oxygen species in the progression of type 2 diabetes and atherosclerosis. Mediators Inflamm. 2010;2010:453892.
9. Bonomini F, Rodella LF, Rezzani R. Metabolic syndrome, aging and involvement of oxidative stress. Aging Dis. 2015;6(2):109-20.
10. Tokarska-Schlattner M, Zaugg M, Zuppinger C, Wallimann T, Schlattner U. New insights into doxorubicin-induced cardiotoxicity: the critical role of cellular energetics. J Mol Cell Cardiol. 2006;41(3):389-405.
11. Granados-Principal S, El-Azem N, Pamplona R, Ramirez-Tortosa C, Pulido-Moran M, Vera-Ramirez L, Quiles JL, et al. Hydroxytyrosol ameliorates oxidative stress and mitochondrial dysfunction in doxorubicin-induced cardiotoxicity in rats with breast cancer. Biochem Pharmacol. 2014;90(1):25-33.
12. Ikeda S, Zablocki D, Sadoshima J. The role of autophagy in death of cardiomyocytes. J Mol Cell Cardiol. 2022;165:1-8.
13. Gao J, Chen X, Shan C, Wang Y, Li P, Shao K. Autophagy in cardiovascular diseases: role of noncoding RNAs. Mol Ther Nucleic Acids. 2020;23:101-118.
14. Sangomla S, Saifi MA, Khurana A, Godugu C. Nanoceria ameliorates doxorubicin induced cardiotoxicity: Possible mitigation via reduction of oxidative stress and inflammation. J Trace Elem Med Biol. 2018;47:53-62.
15. Kumari P, Saifi MA, Khurana A, Godugu C. Cardioprotective effects of nanoceria in a murine model of cardiac remodeling. J Trace Elem Med Biol. 2018;50:198-208.
16. Gupta A. Redox-Active Solid State Materials and its Biomedical and Biosensing Applications. Electronic Theses and Dissertations. University of Central Florida STARS 2017; 5736.
17. Banavar S, Deshpande A, Sur S, Andreescu S. Ceria nanoparticle theranostics: harnessing antioxidant properties in biomedicine and beyond. J Phys Mater. 2021;4(4):42003.
18. Celardo I, Pedersen JZ, Traversa E, Ghibelli L. Pharmacological potential of cerium oxide nanoparticles. Nanoscale. 2011;3(4):1411–20.
19. Hussein AM, Eldosoky M, Handhle A, Elserougy H, Sarhan M, Sobh MA, et al. Effects of long-acting erythropoietin analog darbepoetin-α on adriamycin-induced chronic nephropathy. Int Urol Nephrol. 2016;48(2):287-97.
20. Ibrahim HAM, Hussein AM, Gabr M, El-Saeed RA, Ammar OA, Mosa AAH, Abdel-Aziz AF. Effect of Melatonin on Alpha Synuclein and Autophagy in Dopaminergic Neuronal Differentiation of Adipose Mesenchymal Stem Cells. Rep Biochem Mol Biol. 2023;12(1):13-26.
21. Chacko SM, DhanyaKrishnan R, Nevin KG. Differential Effects of p-Coumaric Acid in relieving Doxorubicin induced Cardiotoxicity in Solid Tumour Bearing and Non-tumor Bearing Mice. J Biol Act Prod from Nature. 2021;11(2):138-61.
22. Wang J, Yao L, Wu X, Guo Q, Sun S, Li J. Protection against Doxorubicin-Induced Cardiotoxicity through Modulating iNOS/ARG 2 Balance by Electroacupuncture at PC6. Oxid Med Cell Longev. 2021;2021:6628957.
23. Podyacheva EY, Kushnareva EA, Karpov AA, Toropova YG. Analysis of Models of Doxorubicin-Induced Cardiomyopathy in Rats and Mice. A Modern View From the Perspective of the Pathophysiologist and the Clinician. Front Pharmacol. 2021;12:670479.
24. Warhol A, George SA, Obaid SN, Efimova T, Efimov IR. Differential

[DOI: 10.61186/rbmb.12.3.495]

cardiotoxic electrocardiographic response to doxorubicin treatment in conscious versus anesthetized mice. Physiol Rep. 2021;9(15):e14987.
25. Salouege I, Ben Ali R, Ben Saïd D, Elkadri N, Kourda N, Lakhal M, Klouz A. Means of evaluation and protection from doxorubicin-induced cardiotoxicity and hepatotoxicity in rats. J Cancer Res Ther. 2014;10(2):274-8.
26. Abdo MELS, Osman AS, Khorshid OA, El-Farouk LO, Kamel MM. Comparative study of the protective effect of metformin and sitagliptin against doxorubicin-induced cardiotoxicity in rats. Clin Pharmacol Biopharm. 2017;6:174.
27. Agaba A, Ebada M, Emara H. Protective Effect of Metformin on Doxorubicin-induced Cardiomyopathy in the Adult Male Albino Rats (Light and Electron Microscopic Study). Al-Azhar Int Med J. 2021;2(4):1-8.
28. Ivanová M, Dovinová I, Okruhlicová L, Tribulová N, Simončíková P, Barteková M, et al. Chronic cardiotoxicity of doxorubicin involves activation of myocardial and circulating matrix metalloproteinases in rats. Acta Pharmacol Sin. 2012;33(4):459-69.
29. Niu J, Azfer A, Rogers LM, Wang X, Kolattukudy PE. Cardioprotective effects of cerium oxide nanoparticles in a transgenic murine model of cardiomyopathy. Cardiovasc Res. 2007;73(3):549-59.
30. Zhou L, Han Y, Yang Q, Xin B, Chi M, Huo Y, et al. Scutellarin attenuates doxorubicin-induced oxidative stress, DNA damage, mitochondrial dysfunction, apoptosis and autophagy in H9c2 cells, cardiac fibroblasts and HUVECs. Toxicol In Vitro. 2022;82:105366.
31. Abdullah CS, Alam S, Aishwarya R, Miriyala S, Bhuiyan MAN, Panchatcharam M, et al. Doxorubicin-induced cardiomyopathy associated with inhibition of autophagic degradation process and defects in mitochondrial respiration. Sci Rep. 2019;9(1):2002.
32. Carrasco R, Castillo RL, Gormaz JG, Carrillo M, Thavendiranathan P. Role of Oxidative Stress in the Mechanisms of Anthracycline-Induced Cardiotoxicity: Effects of Preventive Strategies. Oxid Med Cell Longev. 2021;2021:8863789.
33. Xia P, Chen J, Liu Y, Fletcher M, Jensen BC, Cheng Z. Doxorubicin induces cardiomyocyte apoptosis and atrophy through cyclin-dependent kinase 2-mediated activation of forkhead box O1. J Biol Chem. 2020;295(13):4265-4276.
34. Hosseini M, Mozafari M. Cerium Oxide Nanoparticles: Recent Advances in Tissue Engineering. Materials (Basel). 2020;13(14):3072.
35. Bartlett JJ, Trivedi PC, Pulinilkunnil T. Autophagic dysregulation in doxorubicin cardiomyopathy. J Mol Cell Cardiol. 2017;104:1-8.
36. Dhingra R, Margulets V, Chowdhury SR, Thliveris J, Jassal D, Fernyhough P, et al. Bnip3 mediates doxorubicin-induced cardiac myocyte necrosis and mortality through changes in mitochondrial signaling. Proc Natl Acad Sci U S A. 2014;111(51):E5537-44.
37. Wang X, Wang XL, Chen HL, Wu D, Chen JX, Wang XX, et al. Ghrelin inhibits doxorubicin cardiotoxicity by inhibiting excessive autophagy through AMPK and p38-MAPK. Biochem Pharmacol. 2014;88(3):334-50.
38. Ghotaslou A, Samii A, Boustani H, Kiani Ghalesardi O, Shahidi M. AMG-232, a New Inhibitor of MDM-2, Enhance Doxorubicin Efficiency in Pre-B Acute Lymphoblastic Leukemia Cells. Rep Biochem Mol Biol. 2022;11(1):111-124.
39. Li S, Wang W, Niu T, Wang H, Li B, Shao L, et al. Nrf2 deficiency exaggerates doxorubicin-induced cardiotoxicity and cardiac dysfunction. Oxid Med Cell Longev. 2014;2014:748524.

[DOI: 10.61186/rbmb.12.3.495]

40. Li DL, Wang ZV, Ding G, Tan W, Luo X, Criollo A, et al. Doxorubicin Blocks Cardiomyocyte Autophagic Flux by Inhibiting Lysosome Acidification. Circulation. 2016;133(17):1668-87.
41. Chen Z, Geng Y, Gao R, Zhong H, Chen J, Mu X, et al. Maternal exposure to CeO_2NPs derails placental development through trophoblast dysfunction mediated by excessive autophagy activation. J Nanobiotechnology. 2022;20(1):131.
42. Kawaguchi T, Takemura G, Kanamori H, Takeyama T, Watanabe T, Morishita K, et al. Prior starvation mitigates acute doxorubicin cardiotoxicity through restoration of autophagy in affected cardiomyocytes. Cardiovasc Res. 2012;96(3):456-65.
43. Wang S, Song P, Zou MH. Inhibition of AMP-activated protein kinase α (AMPKα) by doxorubicin accentuates genotoxic stress and cell death in mouse embryonic fibroblasts and cardiomyocytes: role of p53 and SIRT1. J Biol Chem. 2012;287(11):8001-12.
44. Kawaguchi T, Takemura G, Kanamori H, Takeyama T, Watanabe T, Morishita K, Ogino A, et al. Prior starvation mitigates acute doxorubicin cardiotoxicity through restoration of autophagy in affected cardiomyocytes. Cardiovasc Res. 2012;96(3):456-65.
45. Tokarska-Schlattner M, Zaugg M, da Silva R, Lucchinetti E, Schaub MC, Wallimann T, Schlattner U. Acute toxicity of doxorubicin on isolated perfused heart: response of kinases regulating energy supply. Am J Physiol Heart Circ Physiol. 2005;289(1):H37-47.

[DOI: 10.61186/rbmb.12.3.495]